
A Synoptic Parameterization of the Drag Coefficient

Joan Vyverberg Jensen

*Department of Mechanical Engineering
University of Waterloo, Waterloo, Ontario*

[Manuscript received 18 November 1973; in revised form 7 January 1974]

ABSTRACT

The frictional force exerted on the atmosphere over Lake Erie is investigated by incorporating synoptic weather data into boundary layer theory. Over-water data obtained during a severe winter storm by the CCGS N.B. McLean on Lake Erie are used.

The friction force is a function of the drag coefficient C_d . The following expression for C_d is developed which depends primarily on synoptic data: $C_d = f|\vec{V}_g| h V^{-2} \sin \delta$, where δ is the angle between \vec{V} and \vec{V}_g . Drag coefficients were calculated using values of the boundary layer depth h which were

determined from constructed temperature profiles. This depth varies considerably with stability. Approximate values are $h = 0.1$ km for stable, 1 km for neutral, and 1.8 km for unstable conditions.

Drag coefficients over water for unstable conditions appear to be two to ten times larger than for stable circumstances, and are up to eight times the value suggested by Cressman (1960). C_d also varies according to whether it is computed for an over-water, an up-wind or a downwind location.

1 Introduction

Non-adiabatic and windy conditions often prevail during mid-latitude winter storms. The incorporation of these characteristics into numerical prognoses is being studied at the University of Waterloo (Danard, 1971). Frictionally-induced fluxes of sensible heat and water vapour are included in the numerical model as *spatially varying* quantities (Danard and Rao, 1972). The influence of large water bodies is felt through these fluxes, which in turn are dependent on the drag coefficient. These energy flux terms make especially large contributions to the deepening of a storm in locales where a cold air mass comes in contact with a warm body of water. Is the standard value of the drag coefficient for water surfaces, as determined by Cressman (1960), suitable for this situation?

The present study utilizes data obtained on Lake Erie and from surrounding weather stations during the 25–27 January 1971 storm, which was especially severe in the Southern Ontario–Central New York area. These synoptic weather observations are incorporated with boundary layer theory to develop an expression for calculating the drag coefficient. The next section discusses this derivation. The following sections are concerned with the data used and analyses per-

formed, the influence of stability on the boundary layer thickness, and the drag coefficients obtained.

2 Derivation of expression for drag coefficient

The equation governing atmospheric motion can be expressed as

$$\frac{d\vec{V}}{dt} = -\alpha\nabla_H P - f\vec{k} \times \vec{V} + \vec{F} \quad (1)$$

where $d\vec{V}/dt$ is the acceleration of the air parcel, $-\alpha\nabla_H P$ is the horizontal pressure force, $-f\vec{k} \times \vec{V}$ is the Coriolis force and \vec{F} is the friction force, all forces per unit mass. Surface trajectory calculations show that the acceleration term, especially for over-water locations, is small compared with other terms in Eq. (1) and can be ignored. The friction force then balances the pressure and Coriolis forces and must be included in numerical prognoses of storm system development.

Let $\vec{F} = -F\vec{i}$, where \vec{i} is the unit vector directed along the observed surface wind (at 10m); the frictional force is assumed to act oppositely to the surface wind. The magnitude of the friction force may be written

$$F = -\alpha|\nabla_H P| \sin \delta \quad (2)$$

$$F = f|\vec{V}_g| \sin \delta \quad (3)$$

where α is the specific volume, δ is the angle between the geostrophic (\vec{V}_g) and surface (\vec{V}) winds, and f is the Coriolis parameter.

The frictional force is often represented in boundary layer theory by

$$\vec{F} = \frac{1}{\rho} \frac{\partial \vec{\tau}}{\partial z} \quad (4)$$

where $\vec{\tau}$ is the horizontal stress which is assumed to vary linearly with height in the frictional boundary layer. In finite difference form Eq. (4) becomes

$$\vec{F} = \frac{1}{\rho} \frac{\vec{\tau}_h - \vec{\tau}_0}{h} \quad (5)$$

where h is chosen to be the height where the shearing stress due to surface friction becomes negligible, and $z = 0$ for $\vec{\tau}_0$. The surface stress $\vec{\tau}_0$ has the empirically determined form

$$\vec{\tau}_0 = -\rho C_d V^2 \vec{i} \quad (6)$$

where C_d represents the drag coefficient at the height of the observed surface wind.

Setting $\vec{\tau}_h = 0$, combining (5) and (6), and using (3), gives

$$C_d = \frac{f|\vec{V}_g|h \sin \delta}{V^2}. \quad (7)$$

Expression (7) represents the drag coefficient at $z = 10$ m. The assumptions made in deriving this formula imply a simple model of the wind stress caused

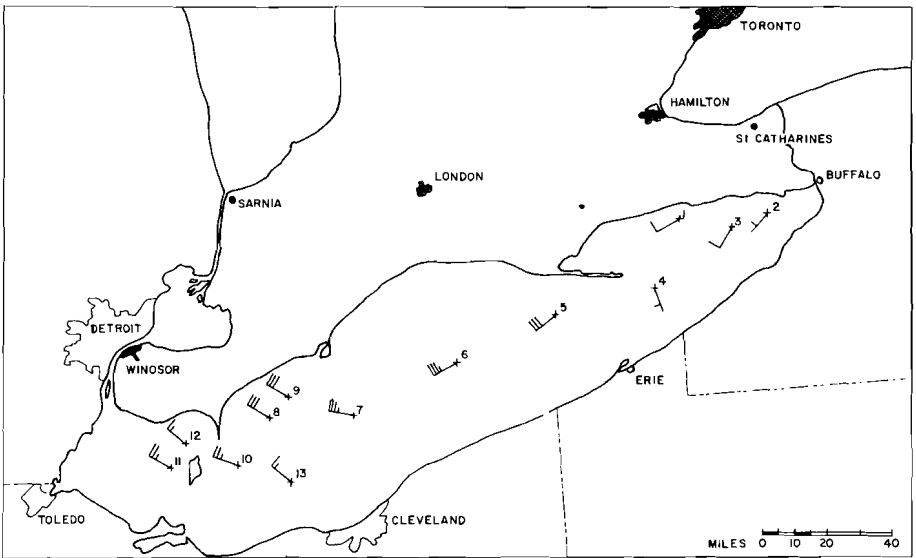


Fig. 1 Location of cgs N.B. McLean on Lake Erie at observation times. Numbers indicate successive positions. Wind speeds shown by full (10 m sec^{-1}) and half (5 m sec^{-1}) barbs.

by friction near the earth's surface. However, Eq. (7) is identical, save for the absence of the thermal wind term, to the "angle equation" of Venkatesh and Csanady (1973). The latter equation is based on a more sophisticated model than that employed in this paper; therefore the similarity of the two equations is encouraging.

3 Initial data and analyses performed

The low-pressure system associated with the storm of 25–27 January 1971 originated east of the Montana Rockies; when over Wisconsin it rapidly developed into an intense winter storm, bringing gale-force winds and heavy drifting to the Lake Erie region and up to 40 cm of snow in the London, Ontario, area (see Fig. 1). During this time, the ice-breaker cgs N.B. McLean was cruising on Lake Erie taking weather observations. The successive locations of the ship are plotted in Fig. 1, as well as the winds observed.

Information from the hourly teletype networks surrounding the Great Lakes was used in conjunction with the ship reports to draw separate streamline and pressure analyses. After the two independent analyses were completed, the maps for each time period were superimposed and the angle δ between the streamlines and isobars was determined for each point where a drag coefficient calculation would be made. The geostrophic wind at that point was also calculated.

Drag coefficients for the N.B. McLean and for near-shoreline locations upwind and downwind of Lake Erie (see Appendix) could then be determined. As a first approximation in these computations, h (the depth of the friction

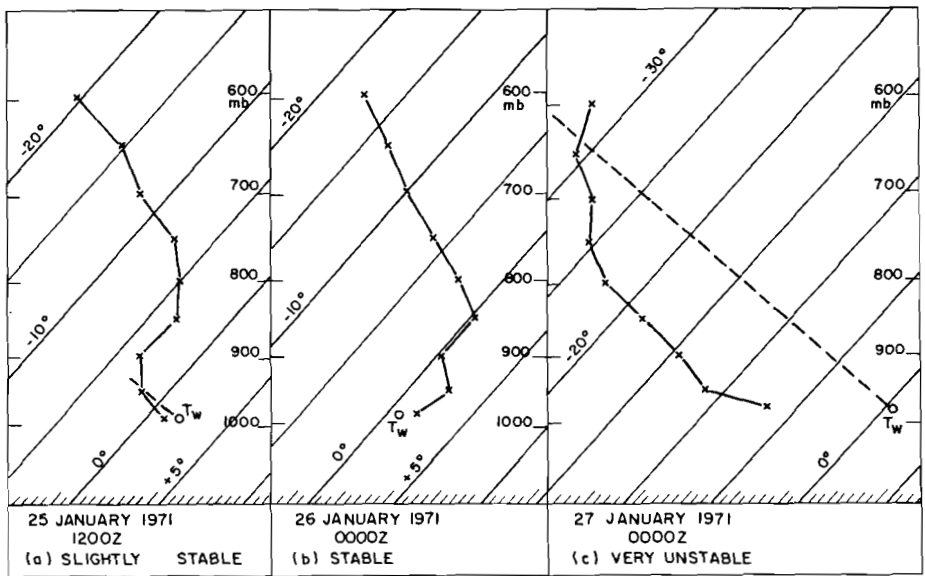


Fig. 2 Temperature soundings constructed for N.B. McLean plotted on tephigram for (a) slightly stable, (b) stable, and (c) very unstable conditions. Temperatures are in degrees Centigrade. Dashed lines in (a) and (c) indicate dry adiabats. Note water temperature (T_w) observed by N.B. McLean compared to surface air temperature (lowest x).

layer) was assumed to equal 1 km in accordance with previous boundary layer studies. However, most theoretical representations of the boundary layer are based on conditions of neutral stability. Therefore an empirical parameterization of the stability in terms of h was developed which could be used in Eq. (7) for the observed non-neutral conditions.

This was done by plotting the upper air temperatures observed at 50 mb intervals (from 950 to 600 mb) by the six radiosonde stations nearest to Lake Erie (SSM, GRB, FNT, PIT, DAY, BUF). The horizontal field was then drawn for each level and temperatures were interpolated for the location of the McLean and of the upwind and downwind stations. These values and the surface air temperature (also water temperature for the McLean) were plotted on a tephigram, giving a reconstructed vertical profile above each point.

Thus three temperature profiles were available for each time. These reconstructed soundings generally gave a clear visual indication of the top of the mixed layer. Specifically, this limit was taken to be the level closest to the earth's surface where the rate of increase of potential temperature became greater than approximately 5°C per 50 mb. For example, in Fig. 2(a) this occurs at 900 mb, in Fig. 2(b) at 985 mb (the surface), in Fig. 2(c) at 650 mb.

4 Influence of stability on boundary layer thickness

Table 1 shows the median values of the boundary layer depth (in km) obtained. The medians include data from the three locations, but are segregated accord-

TABLE 1. Median and range of boundary layer depths.

	Median (km)	Range (km)
Stable	0.1 (estimated)	0.10-0.14
Neutral	0.9	0.87-0.91
Very unstable	1.8	1.63-1.90

TABLE 2. Drag coefficient (C_d) and top of friction layer (h) for land and water locations. Stability categories are: stable (s), neutral (n), unstable (u).

Time	Location	Stability ¹	C_d ($\times 10^{-3}$)	h (km)
12z 25 Jan	Upwind (ERI)	N	31.8	0.90
	McLean	N	3.93	0.91
	Downwind (BUF)	N	2.67	0.87
00z 26 Jan	Upwind (ERI)	s	0.162	0.1 ²
	McLean	s	1.02	0.1 ²
	Downwind (MK)	s	0.236	0.1 ²
12z 26 Jan	Upwind (TOL)	U	39.4	1.63
	McLean	s	0.092	0.14
	Downwind (MK)	s	1.45	0.13
00z 27 Jan	Upwind (DTW)	U	25.1	1.80
	McLean	U	6.15	1.80
	Downwind (CLE)	U	30.6	1.80
12z 27 Jan	Upwind (DTW)	U	29.5	1.90
	McLean	U	4.12	1.89
	Downwind (CLE)	U	125.	1.90

¹McLean stability determined by T_{air} , T_{water} and $\partial\theta/\partial z$ on tephigram; others determined by $\partial\theta/\partial z$ only.

²Entire lower atmosphere was stable. $h = 0.1$ km assumed for sake of computation.

ing to observed low level stability. The range of the depths within each stability category is quite small, as shown in the last column. The small variability may be due to the lack of fine resolution inherent in the procedure used to construct the temperature profiles. However, the disparity between the medians for the *different* stability cases is large. These lake-storm data follow the same trend as the Wangara data (Venkatesh and Csanady, 1973), although here the ratio of unstable to stable values is much larger. Perhaps this is because extremely stormy conditions were prevalent over Lake Erie during the period of observation.

The boundary layer depths (h) determined from the constructed temperature profiles are shown in Table 2, as well as the drag coefficients (C_d) obtained. The strong dependence of h values on stability is particularly noticeable at 12Z 26 January when the upwind station was located in the unstable sector behind the cold front. The McLean and the downwind station were still in the warm stable air.

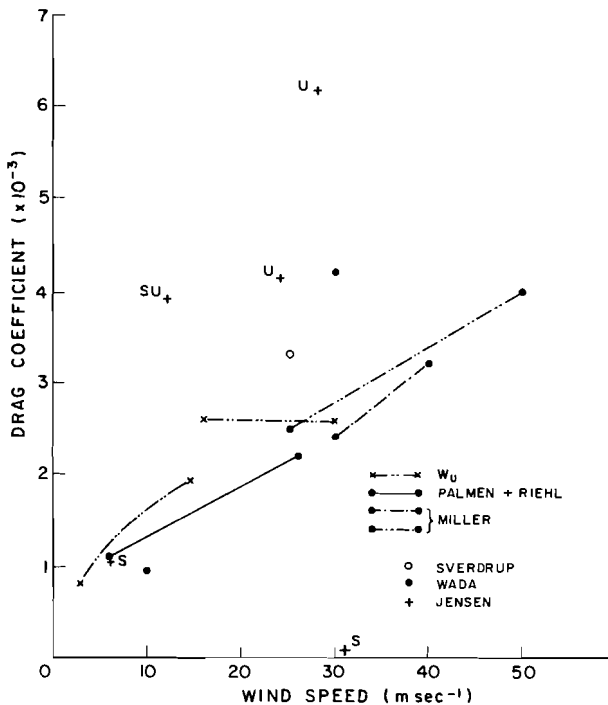


Fig. 3 Drag coefficients as a function of wind speed. Values are for studies conducted during high winds (after Wada, 1969). + indicates values computed in this study from McLean data during times of stable (s), neutral (su) and unstable (u) temperature profiles.

5 Computed drag coefficients

The suitability of the commonly accepted values of the drag coefficient in situations where high winds are observed is questionable. Fig. 3 shows C_d values obtained by Wada (1969) and summarizes her review of other studies which utilize wind velocities approaching typhoon magnitudes. Also on Fig. 3 are the five McLean drag coefficients computed in this study (+). For a given wind speed observed by the McLean, the "unstable" drag coefficients are many times larger than the "stable" values. Note that while individual points are plotted for the Sverdrup, Wada and Jensen studies, the data from other studies have been summarized by one or two lines. Therefore the scatter shown by the separate points is not necessarily inconsistent with results from the other studies. Additional data obtained at high wind speeds and non-neutral stabilities would be helpful in further defining the pattern emerging on Fig. 3.

Table 3 shows the median values for the drag coefficients in Table 2, separated by location and stability. The effect of instability is again very noticeable; however, the variation is opposite in sense to that which might be expected intuitively. This is being studied further.

Because of the small size of the data sample, the derived values of C_d should

TABLE 3. Medians of drag coefficients in Table 2.

Stability	Drag coefficient ($\times 10^{-3}$)		
	Upwind	McLean	Downwind
Stable	0.162	0.55	0.84
Unstable	29.5	5.13	77.8

only be viewed as indicating the order of magnitude. However, the data on Fig. 3 and the medians given in Table 3 imply that for unstable windy conditions the drag coefficient is much higher than the value of 1.2×10^{-3} normally used.

6 Conclusion

Heat and moisture exchanges at the air-earth interface are known to be greater during unstable conditions. Using a variable h when computing the drag coefficient emphasizes the effect of these exchanges. The destabilizing influence of the lakes on downwind locations is shown by the downwind drag coefficients, which are larger by a factor of three than the upwind values. Thus it appears that the exchange terms incorporating the drag coefficient should be adjusted according to land-water location and atmospheric stability. The wind velocity also appears to have a large influence, although extreme variability of wind speeds precludes any systematic categorization in this paper.

Acknowledgements

This research, conducted under the auspices of the Department of Mechanical Engineering, University of Waterloo, with the encouragement of Professor M.B. Danard, was supported by grants from the National Research Council of Canada and the Atmospheric Environment Service.

Preparation of the manuscript was greatly facilitated by Professor R.V. Jones, Department of Natural Philosophy, Aberdeen University, Scotland.

Appendix

Locations of Drag Coefficient Calculations.

Date/Time	McLean Locater Point	Upwind	Downwind
25 January 12z	1	ERI	BUF
26 January 00z	4	ERI	MK
26 January 12z	5	TOL	MK
27 January 00z	9	DTW	CLE
27 January 12z	10	DTW	CLE

References

- CRESSMAN, G.P., 1960: Improved terrain effects in barotropic forecasts. *Mon. Wea. Rev.*, **88**, 327-342.
- DANARD, M.B., 1971: A numerical study of the effects of long-wave radiation and surface friction on cyclone development. *Mon. Wea. Rev.*, **99**, 831-839.
- DANARD, M.B. and G.V. RAO, 1972: Numerical study of the effects of the Great Lakes on a winter cyclone. *Mon. Wea. Rev.*, **100**, 374-382.
- VENKATESH, S. and G.T. CSANADY, 1973: A planetary boundary layer model, and its application to the Wangara data. In press.
- WADA, M., 1969: Concerning the mechanism of the decaying of typhoon. *J. Met. Soc. Japan*, **47**, 335-351.
-